Assessment of Ground Ozone Level under The Physiological Strain Conditions

Robert Krzysztof Sobolewski[1], Robert Kalbarczyk[1]

[1] Wrocław University of Environmental and Life Sciences, Institute of Landscape Architecture, Grunwaldzka 55, 50-357 Wrocław, Poland

* Corresponding author's e-mail: robert.sobolewski.lubawka@gmail.com

ABSTRACT

Urban areas are characterised by the impact of negative environmental factors, such as: stress connected with extreme bio-thermal conditions or the presence of high concentrations of air pollutants. This study aims to evaluate the relationship between the hours of O_3 concentrations and the levels of physiological strain (PhS) in Legnica, during the period from December 2013 to November 2014. The hourly concentrations of O_3, NO_2 and meteorological elements used in the study were obtained from the State Environmental Monitoring station in Legnica (Lower Silesia). The evaluation of the bio-thermal conditions was carried out by means of the physiological strain indicator (PhS). The basic statistics were subject to analysis, the frequency of hourly pollution concentrations and the thermal strain were evaluated, as was the Pearson correlation coefficient and multiple regression between O_3 and PhS. A detailed analysis was carried out for the summer months (June-August). The most adverse conditions in terms of pollution with tropospheric ozone and heat strain were noted in July. The strongest relations between O_3 and PhS were observed in June. In winter months (December-February) no significant dependencies were noted between the tested variables. These tests will help to contribute to increasing the current knowledge on evaluating the thermal comfort of urbanised areas and the accompanying aero-sanitary conditions.

Keywords: air pollution, thermal strain, bioclimate, urban climate

INTRODUCTION

Urban areas modify the atmospheric environment, for instance through the changes of the city's thermal conditions as a result of progressive development and loss of vegetation [Nikolopoulou and Lykoudis 2006, Boumans et al. 2014, van Hove 2015], and changes to air chemistry through the presence of particulate and gas pollution, which includes tropospheric ozone [Carnero et al. 2010]. The tests carried out in Seattle showed an approx. 10% increase in A&E visits caused by asthma attacks along with increased levels of O_3 by each 10 ppb [Goodin, Hubbard 2016]. Additionally, among the children aged 6–15, O_3 and $PM_{2.5}$ particulate lead to a decrease in the lung capacity [Chen et al. 2015]. Novack et al. [2016] showed the impact of air pollution on the oxidative stress of a human body. In their tests, they noted an inverse relation between the high con-

centration of O_3 and a positive relation between suspended particulate PM_{10} and multiplication of blood stem cells. The impact of tropospheric ozone concentration on the respiratory system is confirmed by numerous studies from all over the world: Kinney et al. [1996], Frischer [1999], O'Lenick et al. [2007], Khatri et al. [2001], Tager et al. [2003], Uysal and Schapira [2005]. The research also shows an increase in the death rate by 2% due to hypofunction of the cardiovascular system caused by O_3 pollution on each $10\mu g \cdot m^{-3}$ [Khaniabadi, et al. 2017]. Tropospheric ozone is a secondary pollutant that arises from a series of photochemical reactions [Clapp and Jenkin 2001, Kleinman 2005, Monks et al. 2015, Tiwari et al. 2015]. Moreover, the solar radiation necessary to start the chain reaction, which includes: NO_X ($NO + NO_2$), CO, VOC's and NMVOCs, is absorbed by the human body. The absorption depends on the factors such as: the intensity and

structure of solar radiation, the Sun's altitude (h), ground albedo, body-to-sun orientation and the insulating power and colour of clothing and skin [Błażejczyk 2004]. The highest concentration of O_3 occurs at noon, showing an inverse meridian course from NO_2, NO and NO_x [Escudero et al. 2004, Kalbarczyk et al. 2015, Rozbicka and Rozbicki 2016, Zheng et al. 2017]. In the same hours, the least favourable bio-thermal conditions are observed that impact the human body [Park et al. 2014, Kalbarczyk et al. 2015]. High O_3 concentration is often accompanied by a high air temperature [Vandentorren et al. 2004, Pascal et al. 2012]. Błażejczyk and McGregor [2007], on the basis of 3 bio-thermal indicators: STI, PST, PhS, showed that in London it is possible to explain 20–29% deaths by the certain values of these indicators occuring three days earlier. In Poland, according to Błażejczyka and others [2017], one may expect an increase in mortality on the days characterized by strong and very high heat concentration, with reference to the days when heat stress is observed, by 12% and 47% respectively.

The aim of the study was to evaluate the relationship between the hours of O_3 concentrations and the levels of physiological strain (PhS) in Legnica, during the period from December 2013 to November 2014.

MATERIALS AND METHODS

Legnica is located in the west of Poland, in the Lower Silesia region (51°12′36″N, 16°09′42″E, hs = 113–168 m. a.s.l.). It is the eighth largest (56 km²) and densely populated (1802 people·km⁻²) city in the region and the third largest in terms of population (100886 people) after Wrocław and Wałbrzych **[**Central Statistical Office 2015]. Legnica belongs to the central bioclimatic region of weak stimulusity, characterised by an average air temperature at 12:00 (UTC) of 21.3°C in the summer and 1.9°C in the winter [Błażejczyk and Matzarakis 2007]. This study uses the data of hourly pollution concentrations of O_3, NO_2 and the meteorological data during the period from December 2013 to November 2014. The data was obtained from the State Environmental Monitoring Station in Legnica, marked by the international code PL0190A, indicating a city type station. The data was prepared for universal time (UTC). The initial data verification was carried out on the basis of the correlation between

the O_3 hourly concentration and total radiation (Rad, W·m⁻³), air temperature (Ta, °C), relative air humidity (Rh, %), as well as the wind speed (v, m·s⁻¹) analysis which showed occurrence of two separate data sets. The daily distribution of average values of the meteorological elements showed a sudden drop in the total radiation values between 12:00 and 14:00, depending on the particular month analysed within the researched period, probably caused by the shadowing of the station in the afternoon. The basis of the division into two data sets was the result of carrying out a distribution of average hourly values of meteorological elements for individual decades of each month. The data sets obtained in this way were further used in the correlation analysis.

The evaluation of pollution with the concentrations of O_3 and NO_2 in particular months of the research period was carried out on the basis of descriptive statistics and an analysis of hourly concentration frequencies of O_3 and NO_2 in the adopted classes of pollution levels, consecutively for ozone: 0–40, 41–80, 81–120, >120 µg·m⁻³ and for nitrogen dioxide: 0–20, 21–40, 41–60, 61–80, >80 µg·m⁻³. The evaluation of the bio-thermal conditions was carried out on the basis of the physiological strain (PhS, dimensionless) (Table 1).

The PhS indicator values were calculated by means of the Bioklima 2.6 software (https://www.igipz.pan.pl/Bioklima-zgik.html). The PhS indicator is expressed as the relation of heat loss from a human body by convection (C) to its loss as a result of perspiration evaporation (E) [Błażejczyk, Matzarakis 2007]:

$$PhS = \frac{C}{E} \qquad (1)$$

For each month, there is a frequency related to the occurrence of different concentrations of physiological strain. In turn, the occurrence frequencies of the adopted O_3 concentration in particular classes of physiological strain concentra-

Table 1. Scale of physiological strain (PhS)

PhS	Abbreviation	Scale of physiological strain
< 0.00	EHS	Extreme Hot Strain
0.00 – 0.24	GHS	Great Hot Strain
0.25 – 0.75	MHS	Moderate Hot Strain
0.76 – 1.50	Tn	Thermoneutral
1.51 – 4.00	MCS	Moderate Cold Strain
4.01 – 8.00	GCS	Great Cold Strain
> 8.00	ECS	Extreme Cold Strain

tion were evaluated only for the chosen months characterised by a large and moderate hot strain. For the month of the most frequent extreme conditions in the O_3 concentrations above 120 µg·m⁻³ and hot strain load, an analysis of the daily distribution of O_3, NO_2, values PhS concentration and meteorological elements in subsequent decades was conducted. Due to the asymmetric, right-hand character of the hourly NO_2 concentration schedule, this data was adapted to a normal schedule. In order to do so, the hourly data was stated as a logarithm, which enabled carrying out further statistical analyses. An analysis of the Pearson correlation coefficient between the O_3 and meteorological elements and PhS indicators was carried out for three groups: including the full set of all-day measurements data, morning measurements, that is from sunrise to 13:00 and afternoon measurements data – from 14:00 to sunset. The correlation was evaluated on the level of p=0.05. For the months when the correlation analysis was statistically significant, the equations of multiple regression analyses between tropospheric ozone and conditions of physiological strain in the presence of NO_2 were built.

RESULTS

The descriptive statistics showed that from March to September, the maximum hourly O_3 concentration values in particular months exceeded 127 µg·m⁻³ (Tab. 2) The highest concentration was recorded in July at 159 µg·m⁻³. In turn, the highest NO_2 concentration in the summer period fell in August and was 100 µg·m⁻³. In the same

month, the median value calculated for the NO_2 emission was equal to 15 µg·m⁻³ In the month when the highest O_3 concentration was documented, the value of the PhS indicator amounted to -0.01, which indicates the occurrence of "extreme hot strain" conditions. In the remaining summer months, i.e. June and August, the maximum values of the PhS indicator showed the conditions of "great hot strain". In the winter months (December-February) the maximum monthly O_3 concentration did not exceed 70 µg·m⁻³, the highest recorded in January – 69 µg·m⁻³ In the same month, the maximum value of the PhS indicator amounted to 6.06. This confirms the occurrence of "great cold strain" in this month. The maximum concentration of NO_2 was documented in March at 128 µg·m⁻³; moreover, the maximum concentration above 100 µg·m⁻³ was also recorded in December and February. The value of the third percentile indicates that in July, 25% of all O_3 concentrations were over 98 µg·m⁻³; in comparison, in January, 25% of all concentrations were within the range of 36–64 µg·m⁻³ The highest median values above 50 µg·m⁻³ occurred in July, May, August, June, and April. Thus, the median value for the spring-summer months was higher than the value of the third percentile for winter months.

In July, around 40% of all cases constituted the hourly concentrations above 80 µg·m⁻³; out of that concentration >120 µg·m⁻³ amounted to approx. 11.5% (Fig. 1). March was characterised by the least favourable conditions in terms of the frequencies hourly concentrations of NO_2; the concentrations above 80 µg·m⁻³ constituted 2.8% of recorded cases, in turn, in the scope of 60–80

Table 2. Descriptive statistics for individual months of the research period: Dec. 2013 – Nov. 2014

| Month	Q₁			Me			Q₃			max			min
	O₃	NO₂	PhS	O₃	NO₂	PhS	O₃	NO₂	PhS	O₃	NO₂	PhS	PhS
	µg·m⁻³			µg·m⁻³			µg·m⁻³			µg·m⁻³			
Dec	8	12	2.57	19	26	2.80	42	39	3.03	69	108	4.31	2.01
Jan	8	17	2.68	19	24	3.04	36	33	3.78	64	83	6.06	1.8
Feb	13	13	2.47	39	23	2.78	54	40	3.04	79	106	4.3	1.84
Mar	12	12	2.17	41	20	2.53	60	35	2.84	127	128	3.81	0.86
Apr	25	9	1.77	51	14	2.14	72	24	2.49	128	96	3.2	0.87
May	43	6	1.43	61	10	1.83	78	17	2.17	132	78	3.01	0.31
Jun	39	7	1.13	55	12	1.52	75	19	1.84	153	86	2.39	0.09
Jul	40	8	0.58	67	12	1.06	98	20	1.14	159	79	2.32	-0.01
Aug	32	9	1.01	56	15	1.36	78	25	1.70	139	100	2.37	0.15
Sep	18	12	1.38	37	18	1.65	59	28	1.85	154	92	2.46	0.51
Oct	5	13	1.74	22	21	1.94	43	29	2.36	85	82	3.18	1.00
Nov	3	15	2.23	13	19	2.50	27	26	2.71	70	79	3.43	1.39
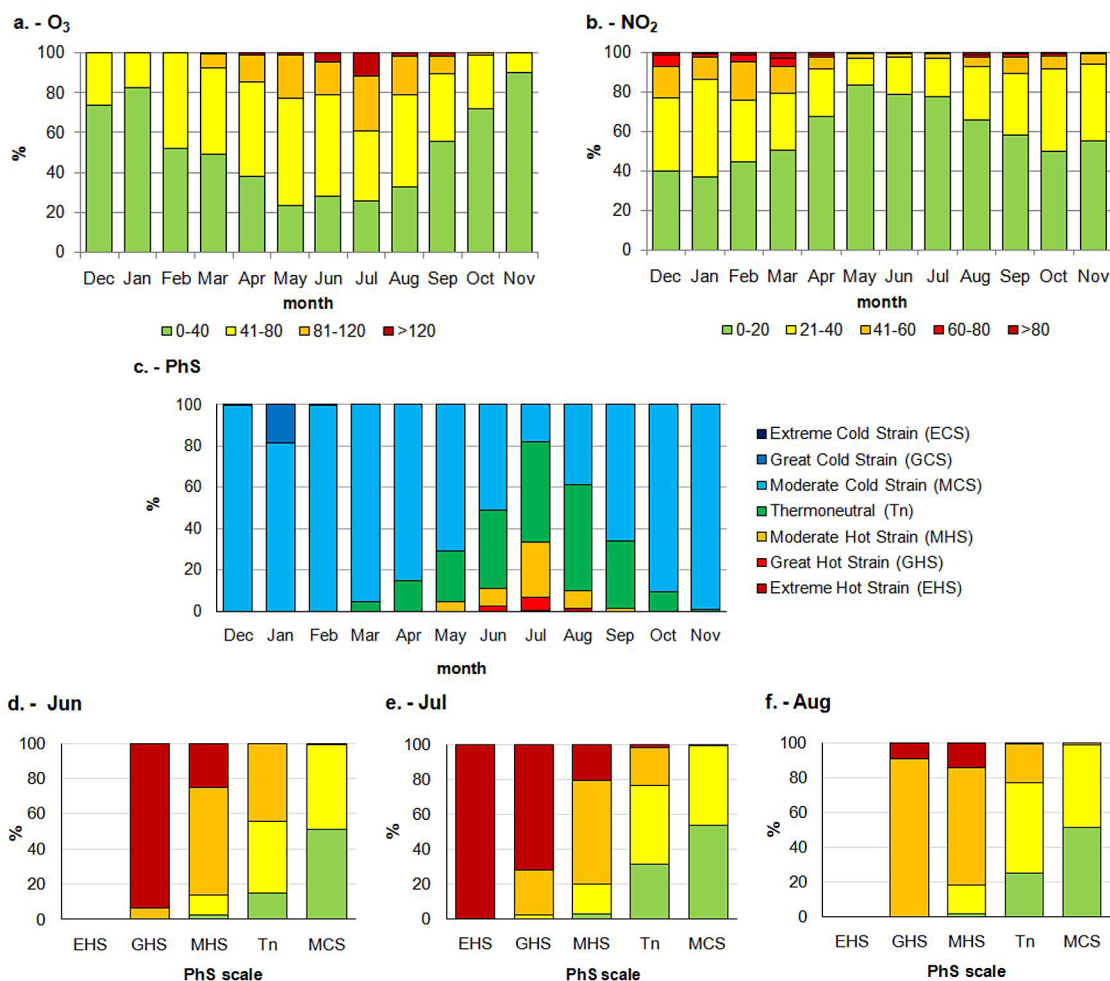
Fig. 1. Occurrence frequencies: the hourly concentrations of gas pollution O_3 and NO_2 (a – b), thermal strain in individual months of the research period (c), and hourly O_3 concentrations in individual classes of physiological strain in June, July, and August (d – f), for the period from December 2013 to November 2014

$\mu g \cdot m^{-3}$ – 4.2%. In July 2014, the conditions connected with hot strain constituted 30% cases. In June and August, the frequencies were comparable, amounting to approx. 11% and 9.7%. In the winter period (December-February), there were almost the same conditions connected with "moderate cold strain", except for January when 18.4% of cases were characterised by "great cold strain". In the remaining months, the strain did not exceed 1%. In the researched period, there were no extreme thermal strain days. Only in July was there a single case of "extreme hot strain". The occurrence of "moderate hot strain" in September was 1.4%, in May approx. 4.5%. The summer period, from June to July, was characterised by the occurrence of thermal conditions from "moderate cold strain" to "extreme hot strain". In July and in June the frequency of O_3 concentrations above 120 $\mu g \cdot m^{-3}$ was connected with the conditions of hot strain. Extreme conditions were re-

corded only in July, which constituted an isolated case. In June, during the "moderate hot strain" approx. 93% cases involved the concentrations above 120 $\mu g \cdot m^{-3}$. In turn, August was characterised by, in comparison to the remaining summer months, a lower frequency of O_3 concentrations above 120 $\mu g \cdot m^{-3}$.

The average hourly O_3 exceeded the value of 100 $\mu g \cdot m^{-3}$ in the second and third decades of July, from 10:00 to 18:00 and from 11:00 to 17:00 (Fig. 2). NO_2 does not show a high changeability of average daily concentration in particular decades. The highest concentration in the second decade was recorded at night. The daily distribution of average O_3 concentrations shows a reverse distribution in reference to the PhS values. The lower values of PhS indicator show the occurrence of the hot strain in the second decade, where the least favourable PhS conditions are recorded, which overlaps with the high level of O_3
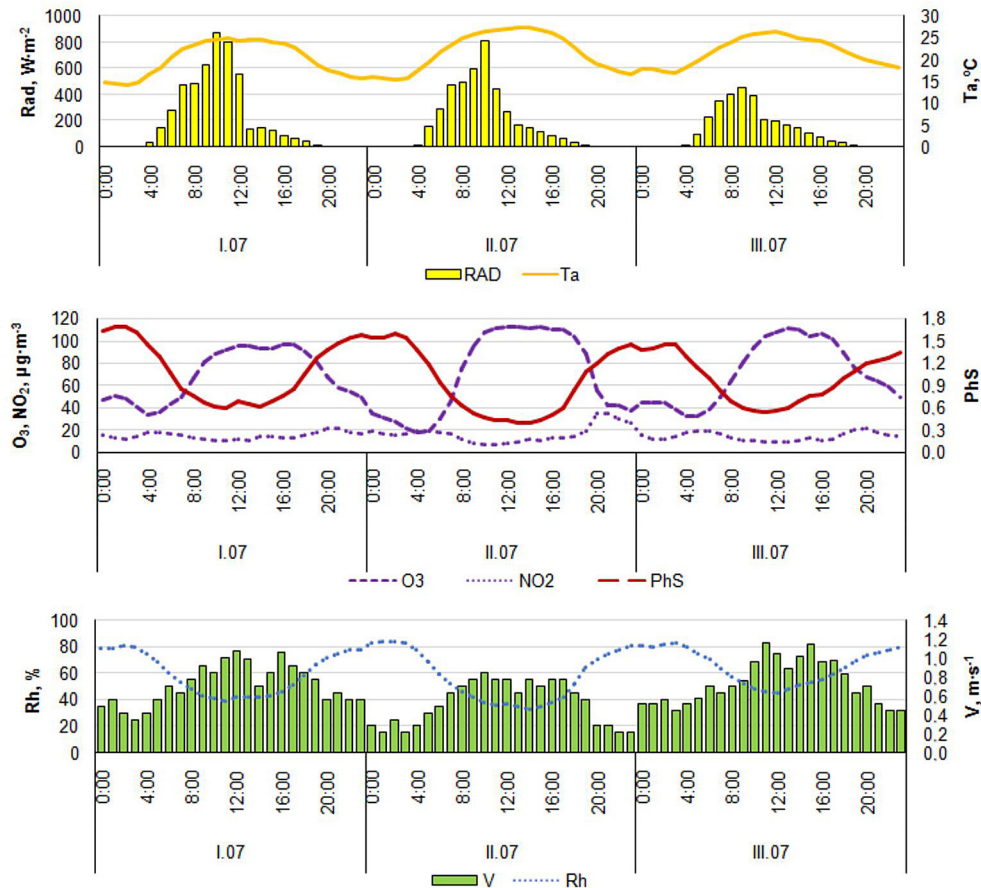
Fig. 2. Daily distribution of average hourly values: O_3, NO_2, PhS and meteorological elements: total radiation Rad, (W·m⁻²) air temperature (Ta, ºC), relative air humidity (Rh, %), wind speed (V, m·s⁻¹) in individual decades of July 2014

concentrations. The solar radiation values show a clear, untypical, drop in the afternoon, which is probably caused by the shadowing of the monitoring station. In the third decade, we can notice a slight increase of the air temperature during the night, which may indicate the effect of the urban heat island present in the research period. The increase of the temperature is accompanied by a slight increase of the tropospheric ozone and the drop in the PhS indicator value.

The maximum hourly O_3 concentrations in July above 150 μg·m⁻³ were recorded between 11:00 and 17:00; they were accompanied by low NO_2 concentrations in the range from 2 to 5 μg·m⁻³ (Tab. 3). From 9:00 to 17:00, the highest hourly O_3 concentrations occurred during significant moderate and great hot strain. Such conditions were favoured by: low relative air humidity below 34%, air temperature above 29°C, and relatively low wind speed approx. 0.7 m·s⁻¹. Only between 8:00 and 10:00, the maximum O_3 concentration was accompanied by solar radiation in the range of 520–713 W·m⁻². At 11:00 total radia-

tion accompanying maximum O_3 values amounted to 219 W·m⁻² and gradually decreased in the following hours. The maximum O_3 concentration amounting to 159 μg·m⁻³ was recorded at 14:00 with the PhS value of 0.09. The least favourable thermal conditions connected with very strong hot strain occurred at 12:00 during the maximum O_3 concentration, amounting to 152 μg·m⁻³.

In the winter period, there was no significant correlation between the hourly O_3 concentrations and the values of the PhS indicator (Tab. 4) A weak correlation (r=0.16, p=0.01) for the data set from 24 h in January constituted an exception. This proven relation has a positive direction, in contrast to the proven relations in the remaining months, which adopted a negative direction (March-November). The reason for the change in the direction of relations between the O_3 concentrations and the PhS values in January could be a lack of correlation between O_3 and Ta for all possible data sets. The strongest, negative relation (r = -0.87, p=0.01) was recorded in June for the afternoon data set, between 14:00 and 19:00, that

Table 3. Maximum O_3 concentration at particular hours of July 2014 in reference to the accompanying meteorological and bio-thermal conditions

Hour	O_3	NO_2 meteorological and physiological strain conditions during the maximum concentration of O_3						PhS	
		NO_2	Rad	Ta	Rh	V	PhS		
	$\mu g \cdot m^{-3}$	$\mu g \cdot m^{-3}$	$W \cdot m^{-2}$	°C	%	$m \cdot s^{-1}$		max	min
00:00	108	8	0	17.9	60	0.7	1.32	2.08	1.04
01:00	109	7	0	18.5	58	1.4	1.36	2.32	1.08
02:00	106	7	0	17.5	62	1.4	1.49	2.17	1.24
03:00	99	8	1	0.0	60	1.4	1.43	2.09	1.04
04:00	92	9	12	18.5	59	1.4	1.37	1.92	1.07
05:00	92	8	28	21.1	53	1.4	1.07	1.81	0.82
06:00	85	9	328	22.4	47	1.4	0.88	1.69	0.44
07:00	96	7	313	24.3	43	1.4	0.69	1.64	0.28
08:00	107	8	520	25.3	39	1.4	0.58	1.49	0.11
09:00	126	7	629	29.5	34	0.7	0.21	1.53	0.1
10:00	148	4	713	30.0	31	0.7	0.18	1.55	0.06
11:00	153	3	219	30.6	29	0.7	0.14	1.68	0.01
12:00	152	5	185	30.9	28	0.7	0.12	1.72	-0.01
13:00	155	5	148	31.5	27	0.7	0.09	1.54	0.02
14:00	159	2	133	31.5	28	0.7	0.09	1.65	0.01
15:00	157	2	106	31.1	28	0.7	0.11	1.59	0.01
16:00	154	4	79	30.7	29	0.7	0.13	1.56	0.04
17:00	152	2	42	29.4	33	1.4	0.23	1.55	0.14
18:00	147	3	26	26.5	42	0.7	0.46	1.58	0.36
19:00	130	11	7	25.0	55	0.7	0.65	1.7	0.56
20:00	121	13	0	23.0	66	0.7	0.88	1.74	0.81
21:00	125	7	0	22.8	64	0.7	0.89	2.08	0.89
22:00	123	8	0	21.1	76	0.7	1.1	2.14	1.06
23:00	114	8	0	18.8	56	0.7	1.21	2.03	1.09

is sunset. For the data from 24 h, the strongest negative correlations in June and July, were r = -0.78 (p=0.01) and r = -0.76 (p=0.01), respectively. In the spring period (March-June) and in September, clear differences in the relations between the morning data sets – from sunrise to 13:00 and in the afternoon – from 14:00 to sunset, were observed. In July and August, the strength of the correlation between O_3 and PhS was comparable both for data from 24 h and from morning and afternoon data sets. In June in the afternoon hours, the strongest correlation between O_3 and Ta (r = 0.90, p=0.01) was observed. The relation between the hourly O_3 concentrations and total radiation for the data set of afternoon measurements in May and June did not show statistical relevancy on the level of p=0.05.

The model of rolling multiple regression was prepared for the months in which there was a significant correlation between O_3 and PhS (Table 5). When examining the model, apart from the PhS indicator, additional hourly NO_2 values in the form of the common logarithm

were taken into account. In the adopted models, significant impact of all changeables explaining the size of O_3 immision was confirmed. The greatest fit of the empirical data to the regression function, amounting to 76% and 80%, was obtained for June, for the conditions in the morning and afternoon; in turn, the smallest fit was observed in April (58%, 43%) and in November (50%, 39%). On the basis of the partial correlation factor, stronger connections between O_3 and bio-thermal conditions, other than NO_2 pollutions were proven in the afternoon hours. In the morning hours, a greater impact of NO_2 on O_3 was recorded, in the prepared model.

DISCUSSION

The research carried out between December 2013 and November 2014 showed a significant relationship between the level of tropospheric ozone and unfavourable bio-thermal conditions connected with hot strain. These relations are

Table 4. Relations between the hourly O_3 concentration and individual meteorological variables as well as the values of the PhS indicator

Month	Period of time	RAD $W \cdot m^{-2}$		Ta °C		Rh %		V $m \cdot s^{-1}$		PhS	
		N	r	N	r	N	r	N	r	N	r
Dec	23:00 – 00:00	743	n.s.	743	0.43***	743	-0.53***	743	0.60***	743	n.s.
	sun rise – 13:00	184	n.s.	184	0.41***	184	-0.52***	184	0.59***	184	n.s.
	14:00 – sun set	48	n.s.	48	0.46***	48	-0.61***	48	0.57***	48	n.s.
Jan	23:00 – 00:00	742	0.19***	742	n.s.	742	-0.60***	742	0.29***	742	0.16***
	sun rise – 13:00	183	0.38***	183	n.s.	183	-0.58***	183	0.14***	183	n.s.
	14:00- sun set	51	0.55***	51	n.s.	51	-0.58***	51	n.s.	51	n.s.
Feb	23:00 – 00:00	666	0.35***	666	0.56***	666	-0.73***	666	0.57***	666	n.s.
	sun rise – 13:00	178	0.43***	178	0.33***	178	-0.66***	178	0.57***	178	n.s.
	14:00 – sun set	74	0.41***	74	0.26***	74	-0.54***	74	0.46***	74	n.s.
Mar	23:00 – 00:00	690	0.31***	690	0.72***	690	-0.64***	690	0.48***	690	-0.61***
	sun rise – 13:00	212	0.52***	212	0.72***	212	-0.65***	212	0.43***	212	-0.60***
	14:00 – sun set	104	0.20***	104	0.59***	104	-0.66***	104	n.s.	104	-0.54***
Apr	23:00 – 00:00	629	0.33***	629	0.54***	629	-0.70***	627	0.51***	627	-0.43***
	sun rise – 13:00	223	0.53***	223	0.45***	223	-0.66***	223	0.35***	223	-0.40***
	14:00 – sun set	111	0.27***	111	0.59***	111	-0.64***	111	n.s.	111	-0.57***
May	23:00 – 00:00	703	0.24***	703	0.60***	703	-0.67***	703	0.50***	703	-0.59***
	sun rise – 13:00	238	0.46***	238	0.53***	238	-0.69***	238	0.43***	238	-0.54***
	14:00 – sun set	186	n.s.	186	0.69***	186	-0.64***	186	0.36***	186	-0.73***
Jun	23:00 – 00:00	665	0.32***	665	0.81***	665	-0.67***	665	0.56***	665	-0.78***
	Sun rise – 13:00	250	0.72***	250	0.78***	250	-0.67***	250	0.45***	250	-0.77***
	14:00 – sun set	186	n.s.	186	0.90***	186	-0.74***	186	0.43***	186	-0.87***
Jul	23:00 – 00:00	740	0.27***	740	0.76***	740	-0.77***	740	0.46***	740	-0.75***
	sun rise – 13:00	271	0.47***	271	0.79***	271	-0.8***	271	0.36***	271	-0.78***
	14:00 – sun set	196	0.20***	196	0.76***	196	-0.64***	196	0.16***	196	-0.75***
Aug	23:00 – 00:00	743	0.37***	743	0.67***	743	-0.68***	743	0.57***	743	-0.66***
	sun rise – 13:00	246	0.61***	246	0.64***	246	-0.71***	246	0.56***	246	-0.67***
	14:00 – sun set	171	0.29***	171	0.65***	171	-0.52***	171	0.38***	171	-0.65***
Sep	23:00 – 00:00	646	0.36***	646	0.65***	646	-0.73***	646	0.60***	646	-0.58***
	sun rise – 13:00	203	0.68***	203	0.68***	203	-0.76***	203	0.57***	203	-0.64***
	14:00 – sun set	118	0.25***	118	0.73***	118	-0.71***	118	0.47***	118	-0.71***
Oct	23:00 – 00:00	741	0.27***	741	0.54***	741	-0.69***	741	0.63***	741	-0.44***
	sun rise – 13:00	203	0.43***	203	0.58***	203	-0.60***	203	0.62***	203	-0.45***
	14:00 – sun set	93	n.s.	93	0.49***	93	-0.63***	93	0.53***	93	-0.31***
Nov	23:00 – 00:00	720	0.27***	720	0.10**	720	-0.75***	720	0.44***	720	-0.26***
	sun rise – 13:00	156	0.44***	156	0.20**	156	-0.75***	156	0.52***	156	-0.42***
	14:00 – sun set	68	0.42***	68	0.29**	68	-0.77***	68	0.43***	68	-0.39***

confirmed by Paliatsos and Nastos [1999] and Matzarakis et al. [2012], who used the thermal discomfort indicator (DI) in their research. Matzarakis et al. [2012] proved the relationship between the O_3 and DI indicators during heat waves (r=0.51, p=0.01). Our research points to stronger relations between O_3 and PhS than DI in June and July, as is evidenced by the correlation factor calculated for both months, r=0.78 (p=0.01) and r=0.75 (p=0.01), respectively. Papanastasiou et al. [2015] on the basis of the discomfort indicator (DI) and CAQI factor, (taking into consideration

pollutants: PM_{10}, NO_2, O_3) showed a deteriorating quality of air during heat waves in Thessaloniki, Athens and Volos in 2001–2010. Kalbarczyk et al. [2016] proved, on the basis of radiation-effective temperature (TRE), a more frequent occurrence of the O_3 concentration levels above $80 \mu g \cdot m^{-3}$ in July and August, when sensing "cold" and "hot" in comparison to other thermal feelings. In April and May, the high level of O_3 concentrations was noted when feeling "comfortable". The relationship between O_3 and NO_2 was the strongest in the winter months; in turn, the strongest impact

Table 5. Equation of the rolling multiple regression between O_3 and NO_2, and PhS for individual months.

Month	Period of time	N	Regression equation			R²adj.	F	Sy	SD	|SD-Sy|
			intercept	regresion coefficient						
				logNO$_2$	PhS			μg·m^{-3}		
Mar	sun rise – 13:00	200	173.35	-55.58	-28.51	0.70	233.32	14.93	26.45	11.52
				-0.58***	-0.52***					
	14:00 – sun set	95	176.92	-47.37	-25.02	0.62	77.07	14.67	23.76	9.09
				-0.58***	-0.61***					
Apr	sun rise – 13:00	219	165.64	-59.7	-20.89	0.58	152.79	18.66	28.67	10.01
				-0.65***	-0.37***					
	14:00 – sun set	111	146.74	-27.46	-21.33	0.43	43.82	14.28	18.95	4.67
				-34***	-0.57***					
May	sun rise – 13:00	236	146.23	-55.88	-18.61	0.56	152.57	16.65	25.12	8.47
				-0.55***	-0.38***					
	14:00 – sun set	181	148.02	-36.78	-21.53	0.63	153.19	16.61	27.04	10.43
				-0.44***	0.43***					
Jun	sun rise – 13:00	248	155.83	-42.74	-44.08	0.76	392.25	14.27	29.4	15.13
				-0.42***	-0.67***					
	14:00 – sun set	185	156.89	-18.86	-49.50	0.80	365.19	12.63	28.2	15.56
				-0.21***	-0.79***					
Jul	sun rise – 13:00	265	172.20	-62.53	-47.95	0.73	348.19	20.18	38.82	18.64
				-0.41***	-0.56***					
	14:00 – sun set	195	161.45	-27.88	-43.38	0.62	160.72	16.85	27.46	10.61
				-0.27***	-0.62***					
Aug	sun rise – 13:00	246	142.10	-45.93	-30.83	0.64	219.96	17.54	29	11.46
				-0.50***	-0.42***					
	14:00 – sun set	171	157.04	-42.57	-26.00	0.67	170.10	13.28	23.17	9.89
				-0.54***	-0.44***					
Sep	sun rise – 13:00	201	176.68	-67.70	-35.04	0.69	227.79	15.00	27.07	12.07
				-0.56***	-0.47***					
	14:00 – sun set	118	217.73	-63.79	-53.04	0.76	186.53	16.12	32.92	16.80
				-0.55***	-0.53***					
Oct	sun rise – 13:00	185	141.90	-64.34	-17.94	0.65	167.80	12.74	21.54	8.8
				-0.67***	-0.35***					
	14:00 – sun set	86	150.98	-58.18	-15.74	0.66	85.51	11.04	20.14	9.10
				-0.76***	-0.3***					
Nov	sun rise – 13:00	130	142.11	-62.60	-19.43	0.50	64.74	13.02	17.92	4.90
				-0.57***	-0.42***					
	14:00 – sun set	60	113.11	-51.54	-16.26	0.39	20.04	13.16	16.43	3.27
				-0.51***	-0.38***					

of tested meteorological elements on the O_3 concentration was recorded in summer. Ramsey et al. [2014] stated that the increase of passable O_3 concentrations during the dry and hot periods can be even three times higher compared to the cold and damp periods. This is confirmed by the occurrence of maximum O_3 concentrations above 150 μg·m^{-3} in Legnica during the times of low relative air humidity below 34% and the air temperature above 29°C. Błażejczyk et al. [2017] ascertained an increase of days >32°C UTCI connected with

the condition of great hot strain between 1966 and 2012, which may have a direct impact on the interactions between the O_3 pollutions and bio-thermal conditions. The results obtained for Legnica indicate that the direct radiation has the least impact on shaping the relations between ozone pollutants and bio-thermal conditions in 2014, despite the documented impact on shaping the level of tropospheric ozone [Clapp, Jenkin 2001, Kleinman 2005, Monks et. al. 2015, Tiwari et al. 2015]. At the turn of the second and third decade

in July, a significant increase of average hourly O_3 concentrations and the loss of average PhS values at night was observed, which could indicate the shaping of the urban heat island effect at that time. Czarnecka and Nidzgorska-Lencewicz [2014] showed a significant connection between the urban heat island in Gdańsk (Poland) and the level of researched pollution concentrations.

CONCLUSIONS

July 2014 was characterised by the least favourable bio-thermal conditions, determined on the basis of the physiological strain indicator (PhS), which were accompanied by an increased risk of occurrence pertaining to the high concentrations of tropospheric ozone above 120 µg·m⁻³ in comparison to the remaining months. These conditions mainly occurred during a significant and moderate hot strain in the afternoon hours, especially in the second decade of the month. Low relative air humidity, high air temperature and weak wind speed had an impact on the deterioration of the bio-thermal conditions and the increase of the O_3 concentration in the summer. Despite the least favourable levels of the O_3 concentrations and PhS values in July, the strongest relations were confirmed in June. The tests carried out may contribute to expanding the current knowledge in the area of thermal comfort evaluation of urban areas and the accompanying aero-sanitary conditions.

Acknowledgements

REFERENCES

1. BioKlima© 2.6., https://www.igipz.pan.pl/Bioklima-zgik.html; 31.09.2016.

2. Błażejczyk A., Błażejczyk, K., Baranowski, J., & Kuchcik, M. 2017. Heat stress mortality and desired adaptation responses of healthcare system in Poland. International Journal of Biometeorology, 1–12.

3. Błażejczyk, K. 2004. Radiation balance in man in various meteorological and geographical conditions. Geographia Polonica, 77(1), 63–76.

4. Błażejczyk K., Matzarakis A. 2007. Assessment of bioclimatic differentiation of Poland, based on the human heat balance. Geographia Polonica, 80(1), 63–82.

5. Boumans R.J., Phillips D.L., Victory W., Fontaine, T.D. 2014. Developing a model for effects of climate change on human health and health–environment interactions: heat stress in Austin, Texas. Urban Climate, 8, 78–99.

6. Carnero J.A., Bolívar J.P., de la Morena B.A. 2010. Surface ozone measurements in the southwest of the Iberian Peninsula (Huelva, Spain). Environmental Science and Pollution Research, 17(2), 355–368.

7. Central Statistical Office 2015, http://stat.gov.pl/; 4.11.2017.

8. Chen, C. H., Chan, C. C., Chen, B. Y., Cheng, T. J., Guo, Y. L. 2015. Effects of particulate air pollution and ozone on lung function in non-asthmatic children. Environmental Research, 137, 40–48.

9. Clapp L. J., Jenkin M. E. 2001. Analysis of the relationship between ambient levels of O_3, NO_2 and NO as a function of NO_x in the UK. Atmospheric Environment, 35(36), 6391–6405.

10. Czarnecka M., Nidzgorska-Lencewicz J. 2014. Intensity of Urban Heat Island and Air Quality in Gdańsk during 2010 Heat Wave. Polish Journal of Environmental Studies, 23(2), 329–340.

11. Escudero M., Lozano A., Hierro J., del Valle J., Mantilla, E. 2014. Urban influence on increasing ozone concentrations in a characteristic Mediterranean agglomeration. Atmospheric Environment, 99, 322–332.

12. Frischer T., Studnicka M., Gartner C., Tauber E., Horak F., Veiter A., Spengler J., Kühr J., Urbanek R. 1999. Lung function growth and ambient ozone: a three-year population study in school children. American Journal of Respiratory and Critical Care Medicine, 160(2), 390–396.

13. Goodin, K., Hubbard M. 2016. Association between asthma hospital visits and ozone concentration in Maricopa County, Arizona (2007–2012). J. Environmental Health, 78(9), 8–13.

14. Kalbarczyk R., Sobolewski R., Kalbarczyk E., 2015: Assessment of human thermal sensations based on bioclimatic indices in a suburban population, Wrocław (SW Poland). Polish Journal of Natural Sciences, 30(2), 185–201.

15. Kalbarczyk R., Sobolewski R., Kalbarczyk E. 2016. Biometeorological determinants of the tropospheric ozone concentration in the suburban conditions of Wroclaw, Poland. Jorunal of Elementology, 21(3), 729–744.

16. Kalbarczyk R., Kalbarczyk E., Niedźwiecka-Filipiak I., Serafin L. 2015. Ozone concentration at ground level depending on the content of NOx and meteorological conditions. Ecological Chemistry

and Engineering S., 22(4), 527–541.

17. Khaniabadi Y.O., Goudarzi G., Daryanoosh S.M., Borgini A., Tittarelli A., De Marco A. 2017. Exposure to PM10, NO2, and O3 and impacts on human health. Environ. Environmental Science and Pollution Research, 24(3), 2781–2789.

18. Khatri S.B., Holguin F.C., Ryan P.B., Mannino D., Erzurum S.C., Teague W.G. 2009. Association of ambient ozone exposure with airway inflammation and allergy in adults with asthma. Journal of Asthma, 46(8), 777–785.

19. Kinney P.L., Thurston G.D., Raizenne, M. 1996. The effects of ambient ozone on lung function in children: a reanalysis of six summer camp studies. Environmental Health Perspectives, 104(2), 170–174.

20. Kleinman L.I. 2005. The dependence of tropospheric ozone production rate on ozone precursors. Atmospheric Environment, 39(3), 575–586.

21. Mavrakis A., Spanou A., Pantavou K., Katavoutas G., Theoharatos G., Christides A., Verouti E. 2012. Biometeorological and air quality assessment in an industrialized area of eastern Mediterranean: the Thriassion Plain, Greece. International Journal of Biometeorology, 56(4), 737–747.

22. Monks P.S., Archibald A.T., Colette A., Cooper O., Coyle M., Derwent R., Fowler D., Granier C., Law K.S., Mills G.E., Stevenson D.S., Tarasova O., Thouret V., von Schneidemesser E., Sommariva R., Wild O., Williams M.L. 2015. Tropospheric ozone and its precursors from the urban to the global scale from air quality to short-lived climate forcer. Atmospheric Chemistry and Physics, 15(15), 8889–8973.

23. Nikolopoulou M., Lykoudis, S. 2006. Thermal comfort in outdoor urban spaces: analysis across different European countries. Building and Environment, 41(11), 1455–1470.

24. Novack L., Yitshak-Sade M., Landau D., Kloog, I., Sarov, B., Karakis I. 2016. Association between ambient air pollution and proliferation of umbilical cord blood cells. Environmental Research, 151, 783–788.

25. O'Lenick C.R., Chang H.H., Kramer M.R., Winquist A., Mulholland J.A. Friberg M.D., Sarnat S. E. 2017. Ozone and childhood respiratory disease in three US cities: evaluation of effect measure modification by neighborhood socioeconomic status using a Bayesian hierarchical approach. Environmental Health, 16(1), 36.

26. Paliatsos A.G., Nastos P.T. 1999. Relation between air pollution episodes and discomfort index in the greater Athens area, Greece. International Journal of Global Nest, 1(2), 91–97.

27. Papanastasiou D.K., Melas D., Kambezidis H.D., 2015. Air quality and thermal comfort levels under extreme hot weather. Atmospheric Research, 152, 4–13.

28. Park S., Tuller S.E., Jo M. 2014. Application of Universal Thermal Climate Index (UTCI) for microclimatic analysis in urban thermal environments. Landscape and Urban Planning 125, 146–155.

29. Pascal M., Wagner V., Chatignoux E., Falq G., Corso M., Blanchard M., Host S., Larrieu S., Laurence P., Declercq, C. 2012. Ozone and short-term mortality in nine French cities: Influence of temperature and season. Atmospheric Environment, 62, 566–572.

30. Ramsey N.R., Klein M.P., Moore III B., 2014. The impact of meterological parameters on urban air quality. Atmos. Environ., 86, 58–67.

31. Rozbicka K., Rozbicki, T. 2016. The "Weekend Effect" on Ozone in the Warsaw Conurbation, Poland. Polish Journal of Environmental Studies, 25(4), 1675–1683.

32. Tager I.B., Balmes J., Lurmann F., Ngo L., Alcorn S., Kunzli N., 2005. Chronic exposure to ambient ozone and lung function in young adults. Epidemiology, 16, 751–759.

33. Tiwari S., Dahiya A., Kumar N. 2015. Investigation into relationships among NO, NO2, NO x, O3, and CO at an urban background site in Delhi, India. Atmospheric Research, 157:,119–126.

34. Uysal N., Schapira, R. M., 2003. Effects of ozone on lung function and lung diseases. Current Opinion in Pulmonary Medicine, 9, 144–150.

35. van Hove L. W.A., Jacobs C.M.J., Heusinkveld B.G., Elbers J.A., van Driel B.L., Holtslag A.A.M. 2015. Temporal and spatial variability of urban heat island and thermal comfort within the Rotterdam agglomeration. Building and Environment, 83, 91–103.

36. Vandentorren S., Suzan F., Medina S., Pascal M., Maulpoix A., Cohen J. C., Ledrans M. 2004. Mortality in 13 French cities during the August 2003 heat wave. American Journal of Public Health, 94(9), 1518–1520.

37. Wolf K., Cyrys J., Harciníková T., Gu J., Kusch T., Hampel R., Schneider A., Peters A. 2017. Land use regression modeling of ultrafine particles, ozone, nitrogen oxides and markers of particulate matter pollution in Augsburg, Germany. Science of the Total Environment, 579, 1531–1540.

38. Zheng S., Singh R.P., Wu Y., Wu C. 2017. A Comparison of Trace Gases and Particulate Matter over Beijing (China) and Delhi (India). Water, Air, & Soil Pollution, 228(5), 181.